

Insights into wind–driven heavy metal pollution and human health risk assessment in a typical lead–zinc mining area of northern China

Zun–zhuang Ke, Xue Han, Ran Zhou, Yi–fei Zhang, Guan–nan Liu, Chang–qing Zhang, Zhao Liu, Xiao–sai Li, Wen–bo Li

Citation: Zun–zhuang Ke, Xue Han, Ran Zhou, Yi–fei Zhang, Guan–nan Liu, Chang–qing Zhang, Zhao Liu, Xiao–sai Li, Wen–bo Li, 2025. Insights into wind–driven heavy metal pollution and human health risk assessment in a typical lead–zinc mining area of northern China, China Geology, 8, 487–499. doi: 10.31035/cg20250039.

View online: https://doi.org/10.31035/cg20250039

Related articles that may interest you

Distributions and risk assessment of heavy metals in solid waste in lead–zinc mining areas and across the soil, water body, sediment and agricultural product ecosystem in their surrounding areas

China Geology. 2025, 8(1), 92 https://doi.org/10.31035/cg2024036

Heavy metal pollution in water and soil and associated health risks in a tin mining region of Hunan Province, Central China

China Geology. 2025, 8(2), 314 https://doi.org/10.31035/cg2023141

Health risk assessment of heavy metals in soils and crops in a mining area (Au–Ag–Cu–trona–oil et al.) of the Nanyang Basin, Henan Province, China

China Geology. 2023, 6(4), 567 https://doi.org/10.31035/cg2022078

Ecological risk assessment and early warning of heavy metal cumulation in the soils near the Luanchuan molybdenum polymetallic mine concentration area, Henan Province, central China

China Geology. 2023, 6(1), 15 https://doi.org/10.31035/cg2023003

Effects of heavy metal pollution on farmland soils and crops: A case study of the Xiaoqinling Gold Belt, China

China Geology. 2020, 3(3), 402 https://doi.org/10.31035/cg2020024

Source analysis and risk evaluation of heavy metal in the river sediment of polymetallic mining area: Taking the Tongl ü shan skarn type Cu–Fe–Au deposit as an example, Hubei section of the Yangtze River Basin, China

China Geology. 2022, 5(4), 649 https://doi.org/10.31035/cg2022052

China Geology 8 (2025) 487−499

China Geology

Journal homepage: http://chinageology.cgs.cn
https://www.sciencedirect.com/journal/china-geology

Insights into wind-driven heavy metal pollution and human health risk assessment in a typical lead-zinc mining area of northern China

Zun-zhuang Ke[a, b], Xue Han[c], Ran Zhou[c], Yi-fei Zhang[c], Guan-nan Liu[a,*], Chang-qing Zhang[a], Zhao Liu[a], Xiao-sai Li[a], Wen-bo Li[b]

[a] *MNR Key Laboratory of Metallogeny and Mineral Assessment, Institute of Mineral Resources, Chinese Academy of Geological Sciences, Beijing* 100037, *China*
[b] *School of Earth and Space Sciences, Peking University, Beijing* 100871, *China*
[c] *No.*1 *Geological institute of China Metallurgical Geology Bureau*

ARTICLE INFO

Article history:
Received 4 February 2025
Received in revised form 10 May 2025
Accepted 16 May 2025
Available online 20 June 2025

Keywords:
Lead-zinc mine
Heavy metals
Health risk
Soil
Semi-arid regions
Vegetable
Wind-driven transport
Food safety
Carcinogenic risk
Sustainable Development Goals (SDG 3)
Environmental geological survey engineering

ABSTRACT

Long-term mining activities can result in the release of heavy metals into soil, ultimately posing a threat to human health. In arid and semi-arid regions, wind-driven transport of these toxic metals from mining areas represents a primary mechanism for their spatial distribution. To evaluate pollution levels and associated health risks of eight metals, A total of 95 soil samples, corresponding 25 vegetable samples and 3 tailing samples were collected from various land types surrounding a typical Pb-Zn mine in northern China's semi-arid region. The mean concentrations of As, Cd, Cr, Cu, Hg, Ni, Pb and Zn in soils were 62.8, 0.27, 29.6, 11.5, 0.02, 14.4, 49.9 and 109.5 mg/kg, respectively. Among these, As, Cd, Pb, and Zn emerged as the predominant pollutants, with some samples exceeding national risk screening values. The results of contamination factor (*CF*), pollution load index (*PLI*) and geo-accumulation index (I_{geo}) indicated that heavy metals in most soils exhibited non-polluted level or slight pollution level, though localized severe contamination by As, Cd, Pb, and Zn was observed. Spatial distribution analysis demonstrated similar dispersion patterns for As, Cd, Pb, and Zn, with wind-mediated transport extending up to 2.0 km from contamination sources. Pearson's correlation analysis and principal component analysis (*PCA*) suggested that As, Cd, Pb and Zn mainly originated from mining activities, and Cr, Ni, Cu and Hg derived from soil parent materials. All vegetable samples contained metal concentrations below food safety thresholds. Health risk assessment showed hazard quotient (HQ) values for individual metals below 1 across all exposure groups, indicating negligible non-carcinogenic risk. Similarly, carcinogenic risk (CR) values for As, Cd, Cr, and Pb fell within acceptable ranges. While mining activities have induced significant localized contamination, the overall affected area remains limited in arid and semi-arid regions. However, greater attention should be directed toward potential health implications from vegetable consumption in proximity to mining operations within arid and semi-arid regions.

©2025 China Geology Editorial Office.

1. Introduction

Global soils were contaminating by heavy metals with economic development and become a significant concern worldwide (Wang FF et al., 2020; Yu JA et al., 2025; Li SL et al., 2024). Approximately 14%–17% of global agricultural land has been affected by toxic metal contamination, exposing an estimated 0.9–1.4 billion people in polluted regions to elevated health risks (Hou DY et al., 2025). According to the 2014 National Soil Pollution Survey of China, heavy metal contamination exceeded regulatory limits at 19.4% of monitored cropland sites, with cadmium surpassing permissible levels at 7.0% of sampling points (Chen NC et al., 2017). Soil heavy metal contamination not only diminishes arable land resources but also poses significant threats to both food security and ecosystem integrity (Munir N et al., 2022). Consequently, soil heavy metal contamination has emerged as a significant barrier to achieving the United Nations' Sustainable Development Goals (SDGs), garnering substantial scientific and policy attention in recent decades (Wang FF et al., 2020; Niu LL et al., 2013; Mazarji M et al., 2021).

First author: *E-mail address*: 2401110638@stu.pku.edu.cn (Zun-zhuang Ke).
* Corresponding author: *E-mail address*: liu.guannan@126.com (Guan-nan Liu).

Literary editor: Xi-jie Chen
doi:10.31035/cg20250039
2096-5192/© 2025 China Geology Editorial Office.

The accumulation of heavy metals in agricultural soils induces physicochemical degradation of soil matrices, impairs nutrient cycling processes, and consequently suppresses crop productivity through multiple pathways (Chu C et al., 2018; Mao CP et al., 2019; Friedlová M, 2010). More critically, heavy metals can be absorbed and accumulated by crops, which may subsequently enter the human body through food consumption, potentially causing adverse effects on human health (Zhang Z et al., 2024; Kumar S et al., 2019; Gergen I and Harmanescu M, 2012). Chronic human exposure to heavy metals may induce carcinogenic effects, chromosomal abnormalities, and heritable genetic mutations through multiple molecular mechanisms (Kim HS et al., 2015; Lan FN et al., 2024; Mishra S et al., 2010).

Although native soils in regions with high geological background levels inherently contain elevated concentrations of heavy metals (Chen LY et al., 2024), the primary source of soil metal pollution stems from anthropogenic activities, such as transportation, industrial operations, agricultural practices and mining activities (Men C et al., 2018 & 2020; Wang FF et al., 2020; Yang SY et al., 2024; Chen DL et al., 2023). In mining areas, long-term mining operations generate a large amount of acid mine drainage (AMD) and tailings (Xie Q et al., 2022; Sun ZH et al., 2018; Demková L et al., 2017; Li ZY et al., 2014; Liang N et al., 2011; Rashed MN, 2010; Wei CY et al., 2009; Chen R et al., 2022; Da Pelo S et al., 2009). The toxic metals present in AMD and airborne dust from tailings can be released into the environment, significantly increasing the concentrations of metal elements in nearly river and soils, leading to severe metal pollution (Qiao PW et al., 2023; Li ZY et al., 2014; Liu HB et al., 2022).

Generally, hydrological dynamics and wind power, which are closely related to climate conditions, play a crucial role in the migration of heavy metals (Pandey B et al., 2014; Yu JY et al., 2024; Liu FL et al., 2024; Liu LH et al., 2020; Zhang YW et al., 2023). In humid regions, the migration of metals is mainly driven by rainfall or surface water (Saha A et al., 2024). Heavy metals existing in dissolved or particulate forms in water can facilitate their long-distance migration. Previous studies have reported that the concentrations of metals in sediments and soils located far from mining areas can also be significantly increased (Chen T et al., 2023; Li ZY et al., 2014; Xie Q et al., 2022; Jian L et al., 2018; Ding Q et al., 2017; Li X et al., 2017). In the semi-arid regions, where annual rainfall is less than 400 mm, the migration of metals via surface water is limited. However, the arid climate exacerbates wind erosion, leading to increased dispersion of tailings containing heavy metals and thus contributing to heavy metal contamination in areas surrounding tailing ponds (Chen T et al., 2023; Khademi H et al., 2018; Mian MH et al., 2004). To date, few studies have focused on the degree and scope of heavy metal pollution driven by wind in arid areas. Hence, it is necessary to investigate the migration of these metallic elements via wind in mining areas of semi-arid regions.

It is remarkable that the semi-arid or arid regions around the world are rich in metal mineral resources, including Australia, China, Chile (Mudd GM et al., 2017). In particular, Pb-Zn ore represents a fundamental metal mineral resource, but metal pollution near Pb-Zn mines is equally serious due to the ultra-high concentrations of Pb, Zn and other multiple associated toxic metals in ores and tailings (Yin ZY et al., 2022; Li ZY et al., 2014). In this study, we selected a typical Pb-Zn mine area located in the semi-arid region of northern China to investigate the migration of wind-driven eight metals and assess their pollution level and health risk associated with vegetable consumption. This study will provide a valuable reference for environmental protection and health risk management in semi-arid regions near mines.

2. Materials and methods

2.1. Study area

The studied Pb-Zn mine is situated in the semi-arid regions of northern China, covering approximately 22 km^2 (Fig. 1a). The mine employs the underground mining methods with dry stack tailings management. The prevailing wind direction is WNW, with an annual mean wind speed of 2.99 m/s (Fig. 1b). The area belonged to the warm temperate zone continental monsoon climate with an annual mean temperature of 2.6°C and mean annual precipitation of 384.5 mm and evaporation of 1625 mm (Fig. 1c). Additionally, the area receives 2897.8 annual sunshine hours.

A small river in the study area exhibits distinct seasonal characteristics, primarily due to scarce rainfall, limited groundwater recharge, and high evaporation rates. The mining area's landform consists of hills ranging in elevation from 1450 to 1700 m, forming a transitional zone between low hills and a plateau. The area's exposed rock types include leptynite, basalt, and volcanic sedimentary rock, with sandy soil predominating.

2.2. Sample collection and pretreatment

A total of 95 soil samples and 25 vegetable samples were collected from the studied area (Fig. 1a). Prior to sample collection, all sampling sites were set by GPS (Fig. 1a). Around mining area was key sampling area (4 km^2) with sampling density of 8–16 samples per square kilometers and outside of mining area (16 km^2) was general sampling area with 2–4 samples per square kilometers. At each sampling site, soil samples were collected using five-point sampling method within a 20-meter radius to ensure representative sampling. Approximately 1 kg of surface soil (0–20 cm) was collected using sample bags. A total of 25 vegetable samples (edible part) were collected at the same soil sample sites, including 23 potato samples, 1 baby cabbage sample and 1 broccoli sample. Additionally, three tailing samples (WK-01, WK-02 and WK-03) were collected from the tailing pond. All collected samples were transported to the laboratory for processing. The dried soil samples and tailings were ground using an agate mortar and sieved through a nylon sieve with 0.149-mm. The processed samples were stored in pre-cleaned polyethylene bottles. The fresh vegetable samples were

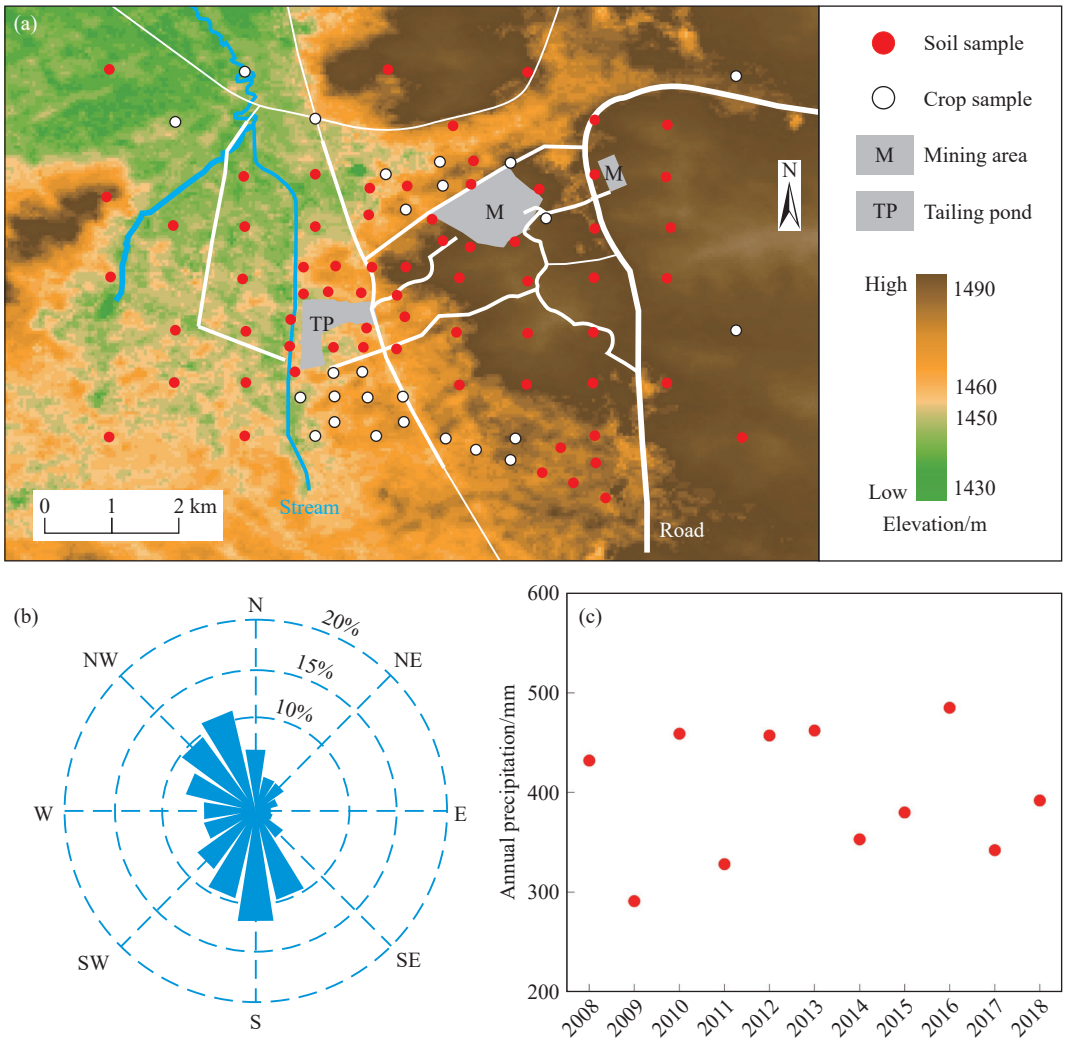


Fig. 1. (a) Digital elevation map (DEM) of the studied area and soil-vegetable sampling locations; (b) the wind rose picture of study area; (c) the annual precipitation of study area (The data from the local meteorological observatory in the studied area).

promptly transferred indoors, cut into small pieces after cleaning with deionized water and then air-dried at 105°C until achieve a constant weight. Finally, the dried samples were then finely ground to powder for subsequent analysis.

2.3. Chemical analysis

The physicochemical properties of all soil samples were characterized, including pH, organic matter (OM), soil particle size (SSZ) distribution, concentrations of metals in soil. Soil pH was measured using a pH meter at a soil-to-water ratio of 1∶2.5. The potassium dichromate redox method was used to measure the concentrations of soil OM. A laser particle analyzer was used to analyze the soil particle size structure composition (Mastersizer-3000, Malvern Instruments Ltd, Britain). For elemental analysis, soil and vegetable samples were digested with HNO_3-$HClO_4$-HF (3∶1∶1, *v/v/v*) and H_2O_2-HNO_3 (1∶1, *v/v*), respectively. Quality control was ensured by analyzing national standard reference materials (GSS-1 and GSS-2 for soils, GSV-1 for vegetables) with each batch of samples. The concentrations of Cd, Cr, Cu, Ni, Pb and Zn in soils were determined by inductively coupled plasma optical emission spectrometer (ICP-OES, Optima 8300, PerkinElmer, Inc., USA). X-ray fluorescence spectrometer (XRF, ZSX Primus Ⅳ, Rigaku-corporation, Japan) was used to measure the concentrations of iron (Fe). The concentrations of As and Hg in soils were measured by atomic fluorescence spectroscopy (AFS, AFS-830, Jitian Instrument Co, Ltd., Beijing). The concentrations of As, Cd, Cr, Cu, Ni, Pb and Zn in vegetables were measured by inductively coupled plasma mass spectrometry (ICP-MS, iCAP^{TM} Q, Thermo, USA), except to Hg in vegetables was measured by AFS (AFS-830, Jitian Instrument Co, Ltd., Beijing).

2.4. Environmental risk assessment

2.4.1. Contamination factor (CF) and pollution load index (PLI)

CF as single factor index was usually used for assessing pollution status of each heavy metals in soil. The relevant calculation formula of *CF* could be as follows formula (1):

$$CF = \frac{C_i}{B_i} \quad (1)$$

Where C_i is concentrations of metal i in soil and B_i is background value of metal i in study area. The soil background values of Hebei province were used, with concentrations of 6.53, 0.11, 40.6, 13.1, 0.02, 15.6, 19.6 and 43.3 mg/kg for As, Cd, Cr, Cu, Hg, Ni, Pb and Zn, respectively (CNEMC, 1990). *CF* values are divided into five levels: non-pollution with $CF<1$, low pollution with $1\leqslant CF<2$, moderate pollution with $2\leqslant CF<3$, high pollution with $3\leqslant CF<5$, extremely high pollution with $5\leqslant CF$.

PLI was used to evaluate overall pollution status for all metals, the *PLI* value obtain from as follow formula (2):

$$PLI = \sqrt[n]{CF_1 \times CF_2 \times \cdots \times CF_n} \tag{2}$$

Where *CF* is contamination factor of each metal, n is the number of types of all metals (n=8). The overall pollution status also could be divided into four levels: low pollution with $PLI<1$, moderate pollution with $1\leqslant PLI<3$, significant pollution with $3\leqslant PLI<6$, very high pollution with $6\leqslant PLI$.

2.4.2. Geo-accumulation index (I_{geo})

I_{geo} played a key role in evaluating pollution level of heavy metals in recent years. The I_{geo} value was calculated as follow formula (3):

$$I_{geo} = \log_2\left(\frac{C_i}{kB_i}\right) \tag{3}$$

Where C_i is concentrations of metal i in soil and B_i is background value of metal i in study area. The k set as 1.5 to avoid metals concentration fluctuation originate from both natural and artificial disturb. According to the calculated I_{geo} results, the contamination levels were divided into seven categories: uncontaminated with $I_{geo}\leqslant 0$, uncontaminated to moderate contaminated with $0\leqslant I_{geo}<1$, moderately contaminated with $1\leqslant I_{geo}<2$, moderately contaminated to heavily contaminated with $2\leqslant I_{geo}<3$, heavily contaminated with $3\leqslant I_{geo}<4$, heavily contaminated to extremely contaminated with $4\leqslant I_{geo}<5$, extremely contaminated with $5\leqslant I_{geo}$.

2.5. Human health risk assessment of consuming vegetables

2.5.1. Mean daily intake (ADI)

ADI of the oral intake pathways can calculate using the following formula (4) (US EPA, 1986, 1989, 2000, 2004):

$$ADI_{food} = C_{food} \times \frac{R_{food} \times AF \times EF \times ED}{AT \times BW} \times 10^{-6} \tag{4}$$

Where ADI_{food} are the mean daily intakes through food by oral intak, mg/(kg·day). C_{food} is the concentrations of heavy metals in vegetable, mg/kg. R_{food} is the food intake rate (150000 and 75000 for adults and children, respectively, mg/day). *AF* is the skin adherence factor (0.20 and 0.07 for adults and children, respectively, mg/cm^2/h). *EF* is the exposure frequency (350 days/year). *ED* is the exposure duration (24 and 6 for adults and children, respectively, years). *AT* is the mean time (*ED*×365 for non-carcinogenic risk and 76.60×365 for carcinogenic risk, days). *BW* is the mean body weight (63 for adults and 29 for children, kg) (Zhang Y et al., 2018).

2.5.2. Hazard quotient (HQ)

HQ was used to calculate the potential non-cancer risk for single intake pathway (US EPA, 1989), the *HQ* could calculate with following formula (5):

$$HQ_i = \sum \frac{\mathrm{A}DI_i}{RfDo_i} \tag{5}$$

$$HI = \sum HQ_i \tag{6}$$

where *ADI* is the mean daily intakes of single pathway; *RfD*o is the reference dose of individual heavy metals for different pathway; *i* stands for the single metal; *j* stands for the pathways; *HI* is the non-carcinogenic risk for multiple pathways (formula (6)). If the *HI* value is equal to or greater than 1, indicated that there is non-carcinogenic risk for adults or children; if the *HI* value is less than 1, there are no significant non-carcinogenic for public. The *RfD* value of As, Cd, Cr, Cu, Hg, Ni, Pb and Zn for ADI_{food} are 0.0003, 0.001, 0.003, 0.04, 0.0003, 0.02, 0.0035 and 0.3 mg/kg/day, respectively, for both adults and children (Cheng Z et al., 2018; Jiang YX et al., 2017; Liu GN et al., 2014).

2.5.3. Cancer risk (CR)

CR was used to assess carcinogenic risk of food intake for public, it could calculate with the following formula:

$$CR_i = ADI_{food} \times SF_o \tag{7}$$

$$TCR = \sum CR_i \tag{8}$$

where *SF*o is the carcinogenic slope factor of oral vegetable intake with dimensionless; *i* stands for the heavy metals. The *SF*o of As, Cr, Cd and Pb for vegetable intake are 1.5, 0.5, 0.0038 and 0.0085 mg/kg/day, respectively (Cheng Z et al., 2018; Chen HY et al., 2016). Hg, Ni, Cu and Zn are not carcinogenic elements in the human body. The *TCR* the sum of *CR*, the results could be divided into three levels: no significant health hazards ($TCR<1\times10^{-6}$), acceptable or tolerable risk ($1\times10^{-6}<TCR<1\times10^{-4}$) and unaccepted risk ($TCR>1\times10^{-4}$).

2.6. Multivariate statistical analysis

Statistical analyses were performed using SPSS version 20.0 (IBM Corp., USA), including Pearson's correlation analysis and principal component analysis (PCA). In the PCA, the principal components were calculated based on the correlation matrix, and Kaiser's standardized orthogonal rotation method was applied to facilitate interpretation of the load matrix. Only those whose default eigenvalue is close to 1 are considered independent components. The spatial distribution pattern of eight metals were visualized using

ArcMap 10.5 (ESRI, USA) with ordinary Krigin interpolation (Acosta JA et al., 2011).

3. Results and discussion

3.1. Soil physicochemical properties

The physicochemical properties of the soils are presented in Table 1. Most soils were sandy, with sand content ranging from 24.8% to 82.9%. Soil pH, which is closely related to bioavailability of heavy metals in soil (Kim RY et al., 2015), varied from 5.87 to 9.41 with large fluctuation. The mean pH of 7.92 indicated the most soils were slightly alkaline, while soils near the mine present low pH values. The observed pH distribution pattern may result from the dispersion and oxidation of dust containing Pb/Zn minerals, such as pyrite (FeS), galena (PbS), and sphalerite (ZnS) (Sun ZH et al., 2018). Soil OM ranged from 4.5% to 83.8%, with a mean value of 20.0±17.2 % and a coefficient of variation of 40.9%, indicating a non-normal distribution. The content of total Fe_2O_3 in soil is between 1.1% and 5.5%, with a mean of 2.4±1.0% and a coefficient of variation of 53.0%, also exhibiting a non-normal distribution. The non-normal distribution of OM and TFe_2O_3 suggest heterogeneous concentration patterns across the studied area.

3.2. Heavy metals in soils, tailings and vegetables

3.2.1. Soil

The concentrations of eight metals in the soils are presented in Table 2. The mean concentrations of Zn, As, Pb, Cr, Ni, Cu, Cd and Hg in soils followed a descending order with mean values of 109.5±196.4, 62.8±295.6, 49.9±121.2, 29.6±12, 14.4±6.7, 11.5±7, 0.27±0.46, and 0.02±0.02 mg/kg, respectively (Fig. 4a). The mean concentrations of As, Cd, Pb and Zn were 9.62, 2.45, 2.55 and 2.53 times of their background values, respectively, and the other metals were close to the background values. The CV of all metals were exceeded 40%, with particularly high values for As (470.6%), Cd (173.9%), Pb (242.7%) and Zn (173.9%). These high CVs indicate heterogeneous or discontinuous spatial distributions of these metals, likely due to strong anthropogenic influences (Wei MC et al., 2023; Xie Q et al., 2022; Wang YZ et al., 2020; Zhao HQ et al., 2023; Zhuo H et al., 2020). Although the mean concentrations of all metals were below their respective risk screening values (GB15618-2018), some individual soil samples exceeded these thresholds for As, Cd, Pb, and Zn. The exceedance rates for these metals were 13.5%, 12.4%, 2.2%, and 6.7%, respectively. Additionally, some samples contained As and Pb at levels surpassing the risk control values. These findings suggest that As, Cd, Pb, and Zn are the primary pollutants in the study area, exhibiting significant contamination. For comparison, previous studies on heavy metal pollution from mining activities were summarized in Table 2. Besides As, Cd, Pb, and Zn, Cr, Cu, and Ni have also been reported to cause moderate to heavy pollution in mining areas in southern China (Table 2). Furthermore, mining-related toxic metal pollution in other countries tends to be more severe than in the study area. Thus, the study area exhibits relatively fewer pollutant types and lower metal concentrations compared to other mining regions.

Table 1. Soil physicochemical properties.

statistic	Sand/%	Silt/%	Clay/%	pH	OM/%	TFe_2O_3/%
Min	24.8	13.5	3.5	5.9	4.5	1.1
Max	82.9	65.5	17.9	9.4	83.8	5.5
Mean	59.5	8.0	32.5	7.9	20.0	2.4
CV/%	23.3	36.2	34.1	8.1	40.9%	53.0

3.2.2. Tailings

The concentrations of eight metals in tailings are presented in Table 3. The mean concentrations of As, Cd, Cr, Cu, Hg, Ni, Pb and Zn were 1219.3±146.0, 5.3±0.7,

Table 2. Heavy metal concentrations in the soils surrounding Pb-Zn mine /(n=89, mg/kg).

Region	Statistical parameters	pH	As	Cd	Cr	Cu	Hg	Ni	Pb	Zn
Studied area	Mean /(mg/kg)	7.92	62.8	0.27	29.6	11.5	0.02	14.4	49.9	109.5
	Max /(mg/kg)	9.41	2146.1	3.21	65.4	57.2	0.15	42.2	1004.4	1541
	Min /(mg/kg)	5.87	3.8	0.03	13.1	4.2	0.01	6.3	15	19.1
	SD	0.65	295.6	0.46	12	7	0.02	6.7	121.2	196.4
	CV /%	8.1	470.6	173.9	40.6	61.2	84.1	46.5	242.7	179.3
	Background values /(mg/kg) (CNEMC, 1990)		6.53	0.11	40.6	13.1	0.02	15.6	19.6	43.3
	Risk screening values /(mg/kg)	6.5<pH<7.5	30	0.3	200	100	2.4	100	120	250
		pH>7.5	25	0.6	250	100	3.4	190	170	300
	RSV exceedance rate/%		13.5	12.4	0	0	0	0	2.2	6.7
Henan, China (Dong Q et al., 2023)		6.5<pH<7.5	30	0.3	200	100	2.4	100	120	250
Village C in Yaoposhan, Guangdong (Sun Z et al., 2018)		4.0-5.7	105	2.51	104	17.86		49.8	681	499
Xikuangshan, Hunan (Li X et al., 2017)		5.50	40.46	7.56	32.30	17.86		18.77	45.43	512.09
Daye, Hubei (Zhou H et al., 2024)			43.25	1.46	90.51	355.72		32.31		260.87
Shangluo, Shannxi (Chen R et al., 2022)		8.5	1257.39	1.43	115.21	39.96	45.14	52.15	20.92	44.37
Nizna Slana, Slovakia (Fazekašová D et al., 2020)		5.7	90.07	0.73	83.15	94.75	1.97	43.73	44.53	114.25
Central Spiš, Slovakia (Demková L et al., 2017)			48.4	1.57	36.98	303.2	11.5	31.77	96.7	482.4
Darreh Zereshk, Iran (Chitsaz M et al., 2021)		8.03	69.42		25.01	36.87		29.25	190.78	170.33

75.9±12.6, 66.4±3.5, 0.041±0.005, 23.7±2.2, 434.0±22.6 and 1578.3±199.1mg/kg, respectively. Notably, the concentrations of As, Cd, Pb, and Zn significantly exceeded the regional soil background values, indicating that these metals in surrounding soils were influenced by mining activities to some extent.

3.2.3. Vegetables

Vegetable samples were collected from farmland within mining regions to determine concentrations of eight metals and assess associated environmental health risks. The concentrations of As, Cd, Cr, Cu, Hg, Ni, Pb and Zn in vegetables were all below China's national food safety limits (GB 2762-2022), with mean values of 0.01±0.00, 0.01±0.00, 0.02±0.01, 0.50±0.18, 0.0005±0.0004, 1.34±0.71, 0.01±0.00, and 2.91±0.92 mg/kg, respectively (Table 4). The bioconcentration factor (*BCF*) is defend as the ratio of bioaccumulated concentrations of toxic metals in plant to the concentrations of toxic metals in rhizosphere soil (Li DX et al., 2022; Ali H et al., 2013; Zhuang P et al., 2007). The descending order of *BCF* was as followed: Ni>Cd>Zn>Cu>Hg>Cr>As>Pb (Fig. S3). BCF analysis revealed no direct correlation between vegetable metal uptake and soil metal concentrations. While some sites had elevated soil metal levels, vegetables demonstrated limited uptake capacity for As, Cd, Pb and Zn. Although toxic metal concentrations in surveyed vegetables were relatively low, long-term consumption may still pose potential health risks (Dong J et al., 2011; Gergen I and Harmanescu M, 2012).

Table 3. Heavy metal concentrations in tailing ponds /(mg/kg).

Tailing	As	Cd	Cr	Cu	Hg	Ni	Pb	Zn
WK-01	1377	4.52	64.1	70.5	0.0401	22.6	454	1362
WK-02	1194	5.95	89.2	64.3	0.0457	26.3	439	1754
WK-03	1088	5.48	74.2	64.4	0.0361	22.3	409	1619
Mean	1219.3	5.30	75.9	66.4	0.041	23.7	434	1578.3
SD	146.0	0.7	12.6	3.5	0.005	2.2	22.6	199.1

3.3. Spatial distribution of pH, TFe_2O_3, OM and heavy metals

The spatial distribution patterns of pH and heavy metals in the study area are presented in Fig. 2. Soil pH represents a key factor controlling the speciation and solubility of heavy metals (Jian L et al., 2018; Li X et al., 2017; Friedlová M,

Table 4. Heavy metal concentrations in vegetables /(n=25, mg/kg).

	As	Cd	Cr	Hg	Ni	Pb	Zn	Cu
Min	2.12×10^{-3}	1.64×10^{-3}	7.36×10^{-3}	6.90×10^{-6}	5.27×10^{-1}	4.40×10^{-3}	1.36×10^{0}	2.72×10^{-1}
Max	1.28×10^{-2}	1.27×10^{-2}	4.40×10^{-2}	1.29×10^{-3}	3.51×10^{0}	1.75×10^{-2}	5.80×10^{0}	1.01×10^{0}
mean	5.46×10^{-3}	6.68×10^{-3}	2.06×10^{-2}	5.35×10^{-4}	1.34×10^{0}	9.87×10^{-3}	2.91×10^{0}	5.04×10^{-1}
SD	2.45×10^{-3}	3.64×10^{-3}	9.96×10^{-3}	3.88×10^{-4}	7.09×10^{-1}	3.36×10^{-3}	9.18×10^{1}	1.83×10^{-1}
CV	4.48×10^{-1}	5.44×10^{-1}	4.84×10^{-1}	7.25×10^{-1}	5.29×10^{-1}	3.41×10^{-1}	3.16×10^{-1}	3.64×10^{-1}

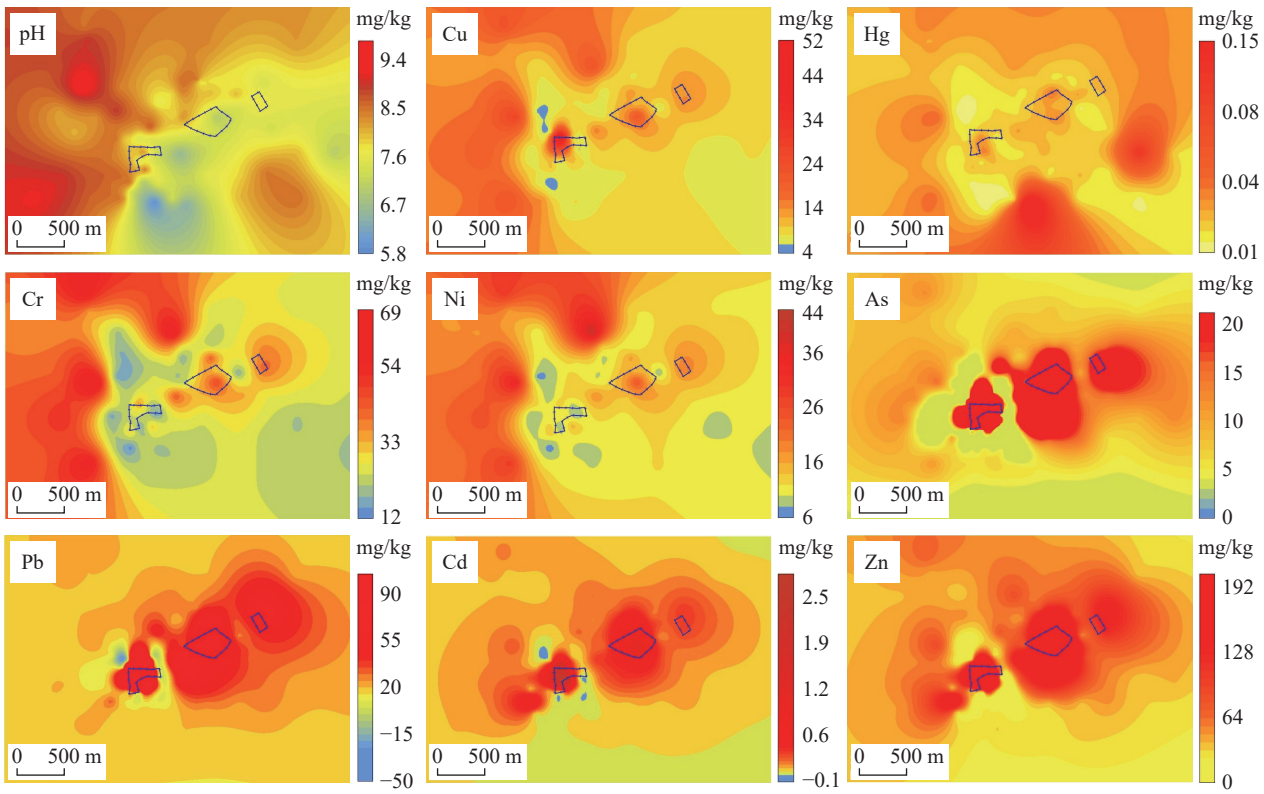


Fig. 2. Spatial distribution characteristics of pH and metals contents in soil.

2010). The study area exhibited a mean soil pH of 7.92, indicating slightly alkaline conditions, while soils in the mining region were acidic. In contrast, the spatial distribution of acidic soils correlated with primary pollutants (As, Cd, Pb, and Zn), suggesting that mining activities induced soil acidification (Feng J et al., 2023; Li ZY et al., 2014; Xie Q et al., 2022). Notably, the spatial distribution patterns of TFe_2O_3 and OM showed a spatial distribution pattern similar to that of pH (Fig. S2).

The spatial distribution patterns of As, Cd, Pb, and Zn showed significant similarity, with elevated concentrations primarily clustered around the tailing pond and mining area (Fig. 2). In contrast, Cr, Ni, and Cu exhibited a distinct west-to-east decreasing gradient, while Hg demonstrated a unique spatial pattern with relatively high concentrations in the southeastern region of the study area. Soil heavy metal pollution usually is spatially heterogeneous due to superposition of multiple pollution sources and accumulation of multi-elements (Wang FF et al., 2020). The similar spatial distribution patterns indicated that those toxic metals with spatial correlativity might be from the same sources (Wang YZ et al., 2020). The consistent spatial distribution patterns of As, Cd, Pb, and Zn, along with their elevated concentrations near the tailing pond and mining area, clearly demonstrate their primary origin from Pb-Zn mining activities. The result also consistent with the concentrations of them in tailings (Table 3). In contrast, Cr, Ni, Cu, and Hg concentrations approximated background levels, suggesting their derivation from natural soil parent materials. Tailings management employs a dry stack process in the Pb-Zn mine. The tailings were transported by auto truck from mining area to tailing ponds. During this transportation process, metal-rich tailings may become dispersed. Furthermore, the study area experiences predominant westerly winds year-round, which facilitate the atmospheric dispersion of metal-bearing particles from both transport operations and tailing ponds, ultimately shaping the observed spatial distribution patterns. Topographic influences also play a crucial role in metal migration (Huang B et al., 2020). The study area's terrain, featuring higher eastern elevations and lower western elevations, effectively restricts the eastward spread of metal-containing dust. This observation aligns well with previous research findings (Ding Q et al., 2017).

The study area is situated in a semi-arid climate zone featuring limited precipitation but abundant wind resources. Consequently, metal migration and dispersion were unlikely attributable to rainfall runoff as observed in humid regions. The wind rose map shows that the main wind direction in the study area is dominated by northwest wind and northwest wind (Fig. 1b). Notably, the spatial distribution pattern of As, Cd, Pb, and Zn follows a distinct southwest-northeast orientation, strongly suggesting that westerly winds primarily drive the transport of these dominant pollutants. Previous studies have demonstrated that wind can effectively mobilize tailings particles and significantly modify their size distribution, with wind speed being a critical factor governing transport dynamics (Stovern M et al., 2015; Huang B et al., 2020, 2014; Ding Q et al., 2017; Yun SW et al., 2017). The dust emission rate of 100 μm tailings increased with the increase in wind speed, potentially causing severe local pollution. In contrast, finer tailings (e.g., 10 μm) can be carried much farther by the wind (Peng XY et al., 2012), the vast majority of Pb-Zn tailings have particle sizes below sand size (<200 μm) (Yang JS et al., 2009). Considering the annual average wind speed (2.99 m/s, Figure 1b), the transport distance of tailings is likely to be restricted. Furthermore, the spatial distribution of primary pollutants indicates that pollution hotspots are limited in extent.

Mining operations, including ventilation systems and ore transportation processes, generate dust containing As, Cd, Pb, and Zn in the atmosphere. Subsequent atmospheric deposition of this metal-laden dust has caused soil enrichment of these elements, leading to As, Cd, Pb, and Zn concentrations that surpass natural background levels in certain areas (Pandey B et al., 2014). In addition, the results of previous studies in mining area show that mining released heavy metals with higher concentrations and the large diffusion areas in other humid and hot area (Table 2). Because humid and hot climatic conditions accelerated the release and leaching of metal elements and enhanced the migration of metal elements (Qiao PW et al., 2023; Liu LH et al., 2020). This study revealed that the spatial distribution of four metals demonstrated a maximum transmission range of approximately 2 km from the core mining area. These findings suggest that heavy metal migration may be more restricted in semi-arid regions compared to humid regions globally. Notably, large deposits of these metals are also found in other semi-arid and arid regions worldwide, including Australia and Chile. The results further imply that wind-driven heavy metal diffusion may similarly occur in these areas. In conclusion, long-term mining activities in these regions have generated heavy metal pollution primarily driven by wind dispersion.

3.4. Source identification of soil heavy metals

Correlation analysis results showed that As exhibited significant positive correlations with Cd, Pb and Zn at the $p<0.01$ significant level (Fig. 3). The correlation coefficients between As and Pb, Zn, Cd were 0.90, 0.77, 0.75, respectively. Similarly, Cr, Ni, Cu and Hg also displayed significant positive correlation with each other at the $p<0.01$ significant level. The results indicated that these elements have the similar pollution sources and diffusion pathway (Xie Q et al., 2022; Li X et al., 2017). A significant negative correlation ($p<0.05$) was observed between pH and Pb. This can be explained by the oxidation of sulfide minerals in tailings, which not only decreases soil pH but also releases heavy metals (Zhang Y et al., 2023). The results indicated that soil Pb was obviously influenced by mining activities. Notably, a lower soil pH can enhance the mobility and bioavailability of most heavy metals, causing them to migrate into deeper soil layers and be absorbed by crops (Chen et al.,

2023). Although, OM can chelate with heavy metals and decrease their mobility and bioavailability as well (Kwiatkowska-Malina J, 2018), it only presented significant and positive correlation with unpolluted elements (Hg, Cr, Ni and Cu, p<0.01). Generally, iron is generally considered a background element due to its naturally high concentrations (Liaghati T et al., 2004). Fe significantly correlated with all elements indicating that a considerable part of these elements were geogenic. In addition, compare with sand and silt composition in soil, the clay composition with Zn and Cd has negative correlation at 0.05 and 0.01 significantly level, respectively. Notably, clay exhibited a negative and significant correlation with Cd and Zn, which were the primary pollutants. While clay has the potential to adsorb more heavy metals due to its high specific surface area, OM, and Fe/Al/Mn oxides (Huang B et al., 2020; Park HJ et al., 2019; Gupta SS, 2005; Lin K et al., 2025), most of the external heavy metals originated from large-particle-sized tailings. Therefore, it is not surprising that clay showed a negative and significant correlation with Cd and Zn. In addition, the clay has stronger adsorption capacity for metals and the clay loaded metals were easily blown away together by the wind (Gupta SS et al., 2005).

Two principal components were extracted from eight metals in Pb-Zn mining area (Table 5; Fig. S1). Two PCs accounted for 82.912% of the total variance, suggesting less information is missing during PCA calculation. The first principal component (PC1) including As, Cd, Pb and Zn can explain 43.165% of the total variance. The Cr, Ni, Cu, Hg and TFe_2O_3 were grouped together accounting for 39.747% of the total variance. The results of principal component analysis were consistent with those of element correlation analysis. In PC1, the sources of As, Cd, Pb, and Zn—identified as the main pollutants in soil—are strongly correlated, indicating their common origin from Pb-Zn mining activities. The spatial distribution of As, Cd, Pb and Zn with high concentrations in mining core regions also affirmed that they originated from mining activities of the Pb-Zn mine. The minerals of the Pb-Zn ore contain galena (PbS), sphalerite (ZnS), arsenic-bearing pyrite (FeAsS) and chalcopyrite ($CuFeS_2$) with high concentrations of Pb, Zn, As and Cd (Zhang CQ et al., 2015; Huang DH et al., 1991). Long-term mining activities lead to

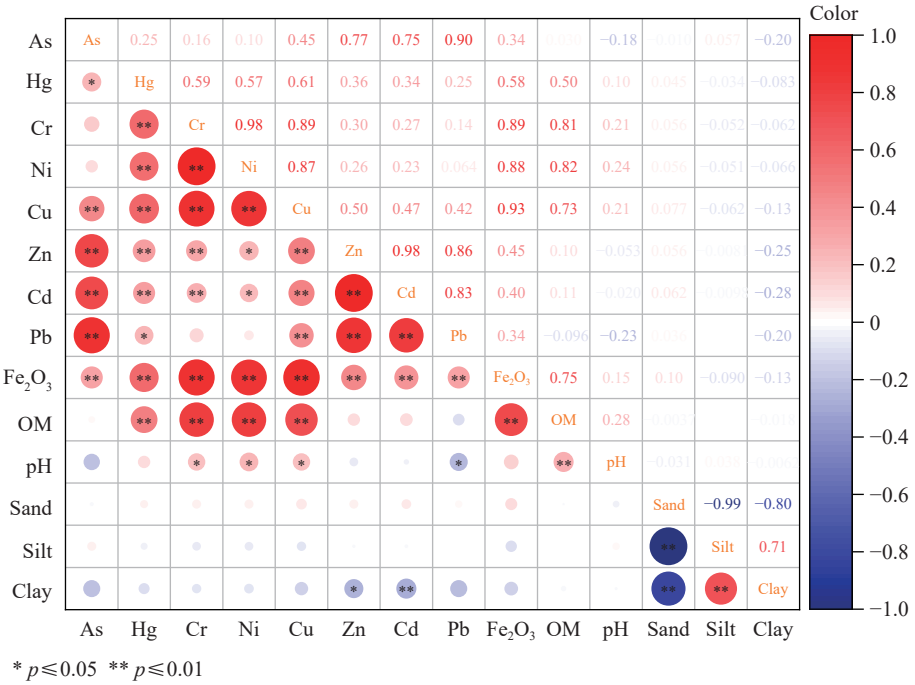


Fig. 3. Pearson's correlation between heavy metals and soil properties.

Table 5. Total variables of soil elements and rotation matrix of PCA.

Component	Initial eigenvalues			Rotation sums of squared loadings			Elements	Component	
	Total	% of variance	Cumulative/%	Total	% of variance	Cumulative/%		1	2
1	4.62	51.33	51.33	3.885	43.165	43.165	As	**0.957**	0.043
2	2.84	31.59	82.91	3.577	39.747	82.912	Cd	**0.947**	0.113
3	0.90	9.95	92.86				Cr	−0.058	**0.981**
4	0.44	4.87	97.73				Cu	0.516	**0.783**
5	0.11	1.25	98.97				Hg	0.099	**0.359**
6	0.05	0.54	99.51				Ni	−0.117	**0.967**
7	0.02	0.27	99.78				Pb	**0.938**	0.130
8	0.01	0.14	99.91				Zn	**0.917**	0.116
9	0.01	0.09	100.00				TFe_2O_3	0.243	**0.945**

the release of As, Cd, Pb and Zn from those crystal ore minerals. In PC2, Cr, Ni, Hg and Cu main from soil parent martial with geological genesis. Although long-term use of pesticides and fertilization with Cu(Ⅱ) leads to the accumulation of metals in farmland soils, the concentrations of Cr, Ni, Cu and Hg in soils and vegetables were smaller than the local background values and the national limit values of toxic metals in food, respectively (Table 2). Therefore, agricultural activities were not the currently source of Cr, Ni, Cu and Hg. The weathering of geological background volcanic rock was mainly contribution to the source of PC2. These results were in agreement with previous studies (Dong Q et al., 2023; Liu GN et al., 2014).

3.5. Environmental risk assessment

The *CF*, I_{geo}, and *PLI* were employed to assess the degree of heavy metal pollution in soils (Fig. 4a~4c). The results showed that the mean *CF* values of As, Cd, Cr, Cu, Hg, Ni, Pb and Zn were 9.19±44.08, 2.44±4.16, 0.72±0.29, 0.87±0.52, 1.06±0.88, 0.92±0.42, 2.49±6.02, and 2.52±4.44 mg/kg, respectively. The mean *CF* values of Cr, Cu, Hg and Ni nearly less than one indicating non-pollution (Fig. 4b). However, the *CF* values of As, Cd, Pb and Zn greater than 2 in mining core area indicated that the soil in Pb-Zn mining region was obviously contaminated by As, Cd, Pb and Zn.

I_{geo} was wildly used to assess the degree of heavy metals pollution in soil or sediment via comparing with geochemical background (Zhuo H et al., 2020). The order of I_{geo} values was followed as: As (0.40±1.52)>Pb (0.03±0.99)>Zn (−0.00±1.23)>Cd (−0.13±1.35)>Hg (−0.73±0.74)>Ni (−0.82±0.56)>Cu (−0.95±0.63)>Cr (−1.15±0.52) (Fig. 4c). The mean I_{geo} values of As and Pb were greater than zero indicating uncontaminated to moderate contaminated level, while other metals were uncontaminated level. In other mining area with higher I_{geo} value were located in southern and eastern of China, the most of the mining areas in southern China are heavily polluted (Li ZY et al., 2014). Although the mean I_{geo} values of all metals were lower than one, the I_{geo} values of some soil samples for As, Cd, Pb and Zn showed heavily contaminated to extremely contaminated level. The I_{geo} results suggested that Pb-Zn mining activities increased the concentrations of As, Cd, Pb and Zn in soil. In additions, the I_{geo} values of some soil samples for Cr, Ni, Cu and Hg in non-mining core area were greater than one, indicating that agricultural activities may cause the pollution in the western part of the study region. Agricultural activities were considered as one of the sources of metals in soil, such as fertilization and spraying pesticides (Sawut R et al., 2018). Hence, agricultural activities may lead to the contents of Cr, Cu, Hg and Zn higher than soil geochemical background. The mean values of *PLI* were 0.88±0.76 indicating a low pollution level (Fig. 4b). The mean *PLI* value less than one suggested that the overall toxic metals pollution level was low.

The studied area is a typical semi-arid area with fragile ecological system (Li PX et al., 2023). Although the current heavy metal (As, Cd, Pb, and Zn) pollution from mining activities in the soil is relatively low, the long-term accumulation of these toxic metals may exacerbate the ecological vulnerability of semi-arid area. Heavy metals in soils can stunt plant growth, inhibit chlorophyll synthesis, degrade local soil quality, and disrupt the soil ecosystem (Chu C et al., 2018; Mao CP et al., 2019). At the same time, long-term consumption of crops containing high concentrations of

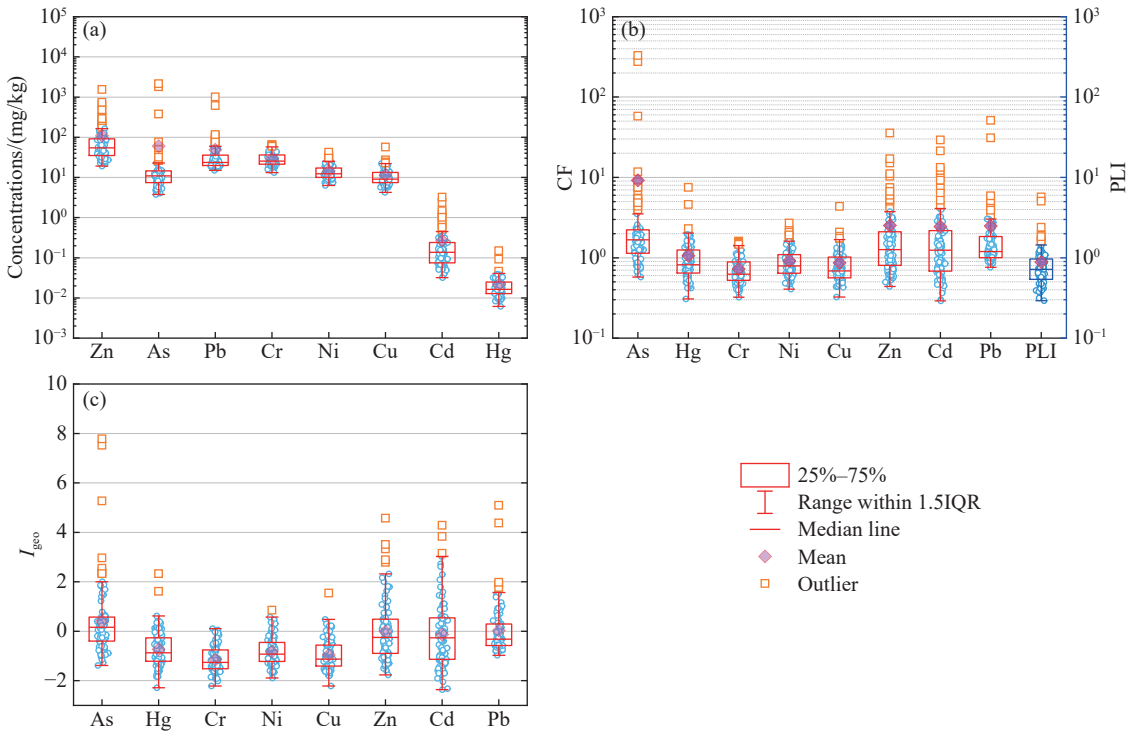


Fig. 4. Boxplots of heavy metal concentrations (a), *CF* and *PLI* (b), I_{geo} (c) in soil.

heavy metals can pose significant risks to human health.

3.6. Human health risk assessment

The *HQ* value was used to assess non-carcinogenic risk effect of eight metals for both adults and children. According to the *HQ* results, the non-carcinogenic risks of Ni and As was higher among the adults and children (Table 6). Hg has the lowest non-carcinogenic risks, lower an order of magnitude than Ni. Except to As, the *HQ* value of adults higher than children, the results suggested that adults should reduce consumption of vegetables, such as potatoes and broccoli. The *HI* value of adults and children were 0.098 and 0.026, respectively. The *HI* value much less than 1, indicating that there is no significant non-carcinogenic risk through oral intake pathway for public. However, the cumulative risk from heavy metals oral intake through vegetable consumption from study area should pay an attention.

The *CR* value was employed to calculate the carcinogenic risk of As, Cd, Cr and Pb for adults and children (Table 6). The *CR* value of As, Cd, Cr and Pb were less than 1×10^{-4}, indicating that the carcinogenic risks for adults and children was acceptable or tolerable. However, the long-term accumulated carcinogenic risk of As, Cd, Cr, and Pb through vegetable consumption should not be ignored.

4. Conclusions

Heavy metals transported by wind represent a significant migration pathway from mine areas in semi-arid regions; however, the extent of their impact may be spatially constrained. This study investigated the influence of mining activities on soils and vegetables, pollution level and human health risk of As, Cd, Cr, Cu, Ni, Hg, Pb and Zn surrounding a Pb-Zn mine in semi-arid region. The main conclusions are as follows:

(i) High concentrations of As, Cd, Pb, and Zn were detected in soils surrounding the mine area, with maximum values reaching 2146.1, 3.21, 1004.4, and 1541.0 mg/kg, respectively. The spatial distribution of these elements extended from the southwest to the northeast, predominantly shaped by wind direction and topographical characteristics. The results of spatial distribution and PCA indicated that As, Cd, Pb, and Zn mainly originated from mining activities. Notably, heavy metal concentrations in vegetables were all below the limit values for food consumption.

(ii) The environmental risk results of *CF*, *PLI*, and I_{geo} indicated that eight metals in most soils exhibited non-polluted level or slight pollution level, except that some soils were severely polluted by As, Cd, Pb and Zn. The *HQs* values of individual metals for the both adults and children were all below one, suggesting a low non-carcinogenic risk. The *CR* value of As, Cd, Cr and Pb were all less than 1×10^{-4}, indicating that the carcinogenic risks for both adults and children from consuming foods near the mine are acceptable or tolerable.

(iii) Although the extent of wind-driven heavy metal pollution is limited in semi-arid areas, extremely high concentrations of toxic metals can still be observed in soils. Therefore, it is crucial to focus on dust suppression from tailings ponds and during the transportation processes of mining activities to prevent further expansion of heavy metal pollution. In addition, the non-carcinogenic and carcinogenic risks associated with long-term consumption of toxic metals contaminated vegetables warrant significant attention. Therefore, it is advisable to avoid cultivating crops or other agricultural products in mine areas and their surrounding regions to mitigate potential human health risks.

Table 6. Non-carcinogenic risks and carcinogenic risks for adults and children.

	Non-carcinogenic risks (HQ)			Carcinogenic risks (CR)	
	Adults	Children		Adults	Children
As	1.43×10^{-2}	3.87×10^{-3}		1.87×10^{-5}	2.03×10^{-5}
Cd	5.23×10^{-3}	1.42×10^{-3}		8.56×10^{-8}	9.30×10^{-8}
Cr	5.37×10^{-3}	1.46×10^{-3}		2.35×10^{-5}	2.55×10^{-5}
Cu	9.87×10^{-3}	2.68×10^{-3}		–	–
Hg	1.40×10^{-3}	3.79×10^{-4}		–	–
Ni	5.25×10^{-2}	1.43×10^{-2}		–	–
Pb	2.21×10^{-3}	5.99×10^{-4}		5.64×10^{-5}	6.13×10^{-5}
Zn	7.58×10^{-3}	2.06×10^{-3}			
HI	9.84×10^{-2}	2.67×10^{-2}	TCR	9.87×10^{-5}	1.07×10^{-4}

CRediT authorship contribution statement

Conceptualization: Guan-nan Liu, Zun-zhuang Ke; Funding acquisition: Chang-qing Zhang, Guan-nan Liu; Investigation: Xue Han, Ran Zhou, Yi-fei Zhang, Guan-nan Liu, Zhao Liu, Xiao-sai Li; Methodology: Guan-nan Liu, Zun-zhuang Ke; Project administration: Chang-qing Zhang, Guan-nan Liu; Visualization-data analysis: Guan-nan Liu, Zun-zhuang Ke; Supervision: Chang-qing Zhang, Guan-nan Liu; Writing–original draft: Zun-zhuang Ke, Guan-nan Liu; Disscuss–review: Guan-nan Liu, Wen-bo Li. All authors read and approved the final manuscript. All authors contributed to the study conception and design.

Declaration of competing interest

The authors declare no conflict to interest.

Acknowledgment

This study was financially supported by the Institute of Mineral Resources, CAGS Research Fund (KK2416), National Natural Science Foundation of China (41807134), China Geological Survey (DD20190182). The author sincerely thanks the two reviewers and chief editor Zi-guo Hao for their constructive suggestions, which have greatly improved the quality and readability of the manuscript.

References

Acosta JA, Faz A, Martínez-Martínez S, Zornoza R, Carmona DM,

Kabas S. 2011. Multivariate statistical and GIS-based approach to evaluate heavy metals behavior in mine sites for future reclamation. Journal of Geochemical Exploration, 109(1–3), 8–17. doi: 10.1016/j.gexplo.2011.01.004.

Ali H, Khan E, Sajad MA. 2013. Phytoremediation of heavy metals—Concepts and applications. Chemosphere, 91(7), 869–881. doi: 10.1016/j.chemosphere.2013.01.075.

Chen DL, Liu GN, Xing ZS, Liu W, Pan FF, Xu JJ, Zhao YY. 2023. Accumulation and source apportionment of soil heavy metals in molybdenum-lead-zinc polymetallic ore concentration area of Luanchuan. Rock and Mineral Analysis, 42(4), 839−851 (in Chinese). doi: 10.15898/j.ykcs.202208090147.

Chen HY, Teng YG, Lu SJ, Wang YY, Wu J, Wang JS. 2016. Source apportionment and health risk assessment of trace metals in surface soils of Beijing metropolitan, China. Chemosphere, 144, 1002–1011. doi: 10.1016/j.chemosphere.2015.09.081.

Chen LY, Ren BZ, Deng XP, Yin W, Xie Q, Cai ZQ, Zou H. 2024. Black shale bedrock control of soil heavy metal typical high geological background in China Loushao Basin: Pollution characteristics, source and Influence assessment based on spatial analysis. Journal of Hazardous Materials, 477, 135072. doi: 10.1016/j.jhazmat.2024.135072.

Chen NC, Zhen YJ, He XF, Zhang XX. 2017. Analysis of the report on the national general survey of soil contamination. Journal of Agro-Environment Science, 36(9), 1689–1692 (in Chinese). doi: 10.11654/jaes.2017-1220.

Chen R, Han L, Liu Z, Zhao YH, Li RS, Xia LF, Fan YM. 2022. Assessment of soil-heavy metal pollution and the health risks in a mining area from southern Shaanxi Province, China. Toxics, 10(7), 385. doi: 10.3390/toxics10070385.

Chen T, Wen XC, Zhou JW, Lu Z, Li XY, Yan B. 2023. A critical review on the migration and transformation processes of heavy metal contamination in lead-zinc tailings of China. Environmental Pollution, 338, 122667. doi: 10.1016/j.envpol.2023.122667.

Cheng Z, Chen LJ, Li HH, Lin JQ, Yang ZB, Yang YX, Xu XX, Xian JR, Shao JR, Zhu XM. 2018. Characteristics and health risk assessment of heavy metals exposure via household dust from urban area in Chengdu, China. Science of the Total Environment, 619, 621–629. doi: 10.1016/j.scitotenv.2017.11.144.

Chitsaz M, Hamidian AH, Moteshare Zadeh B, Dalvand M, Ali Asghar Mirjalili S. 2021. Heavy metals and related properties in farming soils adjacent to a future copper mine, interpretation using GIS, and statistical methods. Arabian Journal of Geosciences, 14(9), 816. doi: 10.1007/s12517-021-06989-5.

Chu CY, Ko TH. 2018. Evaluation of acid leaching on the removal of heavy metals and soil fertility in contaminated soil. Journal of Chemistry, 2018, 5036581. doi: 10.1155/2018/5036581.

CNEMC (China National Environmental Monitoring Center). 1990. The backgrounds of soil environment in china. Beijing, China Environment Science Press 87–496 (in Chinese).

Da Pelo S, Musu E, Cidu R, Frau F, Lattanzi P. 2009. Release of toxic elements from rocks and mine wastes at the Furtei gold mine (Sardinia, Italy). Journal of Geochemical Exploration, 100(2-3), 142–152. doi: 10.1016/j.gexplo.2008.06.006.

Demková L, Jezný T, Bobuľská L. 2017. Assessment of soil heavy metal pollution in a former mining area-before and after the end of mining activities. Soil & Water Research, 12(4), 229–236. doi: 10.17221/107/2016-SWR.

Ding Q, Cheng G, Wang Y, Zhuang DF. 2017. Effects of natural factors on the spatial distribution of heavy metals in soils surrounding mining regions. Science of the Total Environment, 578, 577–585. doi: 10.1016/j.scitotenv.2016.11.001.

Dong J, Yang QW, Sun LN, Zeng Q, Liu SJ, Pan J, Liu XL. 2011. Assessing the concentration and potential dietary risk of heavy metals in vegetables at a Pb/Zn mine site, China. Environmental Earth Sciences, 64(5), 1317–1321. doi: 10.1007/s12665-011-0992-1.

Dong QY, Wen HT, Wang P, Song C, Lai SY, Yang ZJ, Zhao YY, Yan MJ. Health risk assessment of heavy metals in soils and vegetables in a mining area (Au-Ag-Cu-trona-oil et al.) of the Nanyang Basin, Henan Province, China. China Geology, 2023, 6(4), 567-579. doi:10.31035/cg2022078.

Fazekašová D, Fazekaš J. 2020. Soil quality and heavy metal pollution assessment of iron ore mines in nizna slana (Slovakia). Sustainability, 12(6), 2549. doi: 10.3390/su12062549.

Feng J, Ai H, Chen QM, Li H, Wang WB, Xue ZF. 2023. Evaluation and migration path analysis of soil heavy metal pollution in a metal mining area of Qinling Mountain. Rock and Mineral Analysis, 42(6), 1189−1202 (in Chinese). doi:10.15898/j.ykcs.202302170021.

Friedlová M. 2010. The influence of heavy metals on soil biological and chemical properties. Soil & Water Research, 5(1), 21–27. doi: 10.17221/11/2009-swr.

Gergen I, Harmanescu M. 2012. Application of principal component analysis in the pollution assessment with heavy metals of vegetable food chain in the old mining areas. Chemistry Central Journal, 6(1), 156. doi: 10.1186/1752-153X-6-156.

Gupta SS, Bhattacharyya KG. 2005. Interaction of metal ions with clays: I. A case study with Pb(II). Applied Clay Science, 30(3-4), 199–208. doi: 10.1016/j.clay.2005.03.008.

Hou DY, Jia XY, Wang LW, McGrath SP, Zhu YG, Hu Q, Zhao FJ, Bank MS, O'Connor D, Nriagu J. 2025. Global soil pollution by toxic metals threatens agriculture and human health. Science, 388(6744), 316–321. doi: 10.1126/science.adr5214.

Huang B, Li ZW, Huang JQ, Guo L, Nie XD, Wang Y, Zhang Y, Zeng GM. 2014. Adsorption characteristics of Cu and Zn onto various size fractions of aggregates from red paddy soil. Journal of Hazardous Materials, 264, 176–183. doi: 10.1016/j.jhazmat.2013.10.074.

Huang B, Yuan ZJ, Li DQ, Zheng MG, Nie XD, Liao YS. 2020. Effects of soil particle size on the adsorption, distribution, and migration behaviors of heavy metal(loid)s in soil: A review. Environmental Science Processes & Impacts, 22(8), 1596–1615. doi: 10.1039/d0em00189a.

Huang DH, Ding XS, Wu CY, Zhang CJ. 1991. Mineral characteristics and occurrence of gold, silver and bismuth of the Caijiaying lead-zinc-silver deposit, Hebei province. Acta Geological Sinica, 65(2), 127–140,201 (in Chinese). doi: 10.19762/j.cnki.dizhixuebao.1991.02.003.

Jian L, Jiao WB, Qiu HY, Chen B, Huang XX, Kang B. 2018. Origin and spatial distribution of heavy metals and carcinogenic risk assessment in mining areas at You'xi County south East China. Geoderma, 310, 99–106. doi: 10.1016/j.geoderma.2017.09.016.

Jiang YX, Chao SH, Liu JW, Yang Y, Chen YJ, Zhang AC, Cao HB. 2017. Source apportionment and health risk assessment of heavy metals in soil for a township in Jiangsu Province, China. Chemosphere, 168, 1658–1668. doi: 10.1016/j.chemosphere.2016.11.088.

Khademi H, Abbaspour A, Martínez-Martínez S, Gabarrón M, Shahrokh V, Faz A, Acosta JA. 2018. Provenance and environmental risk of windblown materials from mine tailing ponds, Murcia, Spain. Environmental Pollution, 241, 432–440. doi: 10.1016/j.envpol.2018.05.084.

Kim HS, Kim YJ, Seo YR. 2015. An overview of carcinogenic heavy metal: Molecular toxicity mechanism and prevention. Journal of Cancer Prevention, 20(4), 232–240. doi: 10.15430/JCP.2015.20.4.232.

Kim RY, Yoon JK, Kim TS, Yang JE, Owens G, Kim KR. 2015. Bioavailability of heavy metals in soils: Definitions and practical implementation —A critical review. Environmental Geochemistry and Health, 37(6), 1041–1061. doi: 10.1007/s10653-015-9695-y.

Kumar S, Prasad S, Yadav KK, Shrivastava M, Gupta N, Nagar S, Bach QV, Kamyab H, Khan SA, Yadav S, Malav LC. 2019. Hazardous heavy metals contamination of vegetables and food chain: Role of sustainable remediation approaches - A review. Environmental Research, 179, 108792. doi: 10.1016/j.envres.2019.108792.

Kwiatkowska-Malina J. 2018. Functions of organic matter in polluted soils: The effect of organic amendments on phytoavailability of heavy metals. Applied Soil Ecology, 123, 542–545. doi: 10.1016/j.apsoil.2017.06.021.

Lan FN, Zhao Y, Li J, Zhu XQ. 2024. Health risk assessment of heavy metal pollution in groundwater of a Karst basin, SW China. Journal of Groundwater Science and Engineering, 12(1), 49–61 doi: 10.26599/jgse.2024.9280005.

Li DX, Liu GN, Li XS, Li RP, Wang J, Zhao YY. 2022. Heavy metal(loid)s pollution of agricultural soils and health risk assessment of consuming soybean and wheat in a typical non-ferrous metal mine area in North East China. Sustainability, 14(5), 1–15. doi: 10.3390/su14052953.

Li PX, Wang B, Chen P, Zhang YL, Zhao SH. 2023. Vulnerability assessment of the eco-geo-environment of mining cities in arid and semi-arid areas: A case study from Zhungeer, China. Ecological Indicators, 152, 110364. doi: 10.1016/j.ecolind.2023.110364.

Li SL, Wang H F, Liu J, Zhang A B, Wei K H, Li B. 2024. Risk assessment and influencing factors analysis of heavy metals in soil of non-surface coal mines in southern Hebei Province. Rock and Mineral Analysis, 43(5), 769−782 (in Chinese). doi: 10.15898/j.ykcs.202401180006.

Li X, Yang H, Zhang C, Zeng GM, Liu YG, Xu WH, Wu YE, Lan SM. 2017. Spatial distribution and transport characteristics of heavy metals around an antimony mine area in Central China. Chemosphere, 170, 17–24. doi: 10.1016/j.chemosphere.2016.12.011.

Li ZY, Ma ZW, van der Kuijp TJ, Yuan ZW, Huang L. 2014. A review of soil heavy metal pollution from mines in China: Pollution and health risk assessment. Science of the Total Environment, 468, 843–853. doi: 10.1016/j.scitotenv.2013.08.090.

Liaghati T, Preda M, Cox M. 2004. Heavy metal distribution and controlling factors within coastal plain sediments, Bells Creek catchment, southeast Queensland, Australia. Environment International, 29(7), 935–948. doi: 10.1016/S0160-4120(03)00060-6.

Liang N, Yang LY, Dai JR, Pang XG. 2011. Heavy metal pollution in surface water of Linglong gold mining area, China. Procedia Environmental Sciences, 10, 914–917. doi: 10.1016/j.proenv.2011.09.146.

Lin K, Li B, Guan DX, Wu ZL, Li XZ, Ji WB, Liu W, Yu T, Yang ZF. 2025. Enrichment mechanisms of cadmium in natural manganese-rich nodules from Karst soils. Environmental Science & Technology, 59(14), 7256–7267. doi: 10.1021/acs.est.4c11918.

Liu FL, Liu Z, Gao Y, Liu R, Wang DM, Wang BM, You Y. 2024. Migration pathway and solidification mechanism of heavy metal Pb during the conversion of municipal solid waste incineration fly ash into ettringite and simultaneously purification of chloride salts solution process. Environmental Pollution, 341, 122859. doi: 10.1016/j.envpol.2023.122859.

Liu GN, Yu YJ, Hou J, Xue W, Liu XH, Liu YZ, Wang WH, Alsaedi A, Hayat T, Liu ZT. 2014. An ecological risk assessment of heavy metal pollution of the agricultural ecosystem near a lead-acid battery factory. Ecological Indicators, 47, 210–218. doi: 10.1016/j.ecolind.2014.04.040.

Liu HB, Qu MK, Chen J, Guang X, Zhang JL, Liu MS, Kang JF, Zhao YC, Huang B. 2022. Heavy metal accumulation in the surrounding areas affected by mining in China: Spatial distribution patterns, risk assessment, and influencing factors. Science of the Total Environment, 825, 154004. doi: 10.1016/j.scitotenv.2022.154004.

Liu LH, Ouyang W, Wang YD, Tysklind M, Hao FH, Liu HB, Hao X, Xu YX, Lin CY, Su LY. 2020. Heavy metal accumulation, geochemical fractions, and loadings in two agricultural watersheds with distinct climate conditions. Journal of Hazardous Materials, 389, 122125. doi: 10.1016/j.jhazmat.2020.122125.

Mao CP, Song YX, Chen LX, Ji JF, Li JZ, Yuan XY, Yang ZF, Ayoko GA, Frost RL, Theiss F. 2019. Human health risks of heavy metals in paddy rice based on transfer characteristics of heavy metals from soil to rice. Catena, 175, 339–348. doi: 10.1016/j.catena.2018.12.029.

Mazarji M, Bayero MT, Minkina T, Sushkova S, Mandzhieva S, Tereshchenko A, Timofeeva A, Bauer T, Burachevskaya M, Kızılkaya R, Gülser C, Keswani C. 2021. Realizing united nations sustainable development goals for greener remediation of heavy metals-contaminated soils by biochar: Emerging trends and future directions. Sustainability, 13(24), 13825. doi: 10.3390/su132413825.

Men C, Liu RM, Wang QR, Guo LJ, Shen ZY. 2018. The impact of seasonal varied human activity on characteristics and sources of heavy metals in metropolitan road dusts. Science of the Total Environment, 637, 844–854. doi: 10.1016/j.scitotenv.2018.05.059.

Men C, Liu RM, Xu LB, Wang QR, Guo LJ, Miao YX, Shen ZY. 2020. Source-specific ecological risk analysis and critical source identification of heavy metals in road dust in Beijing, China. Journal of Hazardous Materials, 388, 121763. doi: 10.1016/j.jhazmat.2019.121763.

Mian M H, Yanful E K. 2004. Analysis of wind-driven resuspension of metal mine sludge in a tailings pond. Journal of Environmental Engineering and Science, 3(2), 119–135. doi: 10.1139/S03-076.

Mishra S, Dwivedi S P, Singh R B. 2010. A review on epigenetic effect of heavy metal carcinogens on human health. The Open Nutraceuticals Journal, 3(1), 188. doi: 10.2174/1876396001003010188.

Mudd GM, Jowitt SM, Werner TT. 2017. The world's lead-zinc mineral resources: Scarcity, data, issues and opportunities. Ore Geology Reviews, 80, 1160–1190. doi: 10.1016/j.oregeorev.2016.08.010.

Munir N, Jahangeer M, Bouyahya A, El Omari N, Ghchime R, Balahbib A, Aboulaghras S, Mahmood Z, Akram M, Ali Shah SM, Mikolaychik IN, Derkho M, Rebezov M, Venkidasamy B, Thiruvengadam M, Ali Shariati M. 2022. Heavy metal contamination of natural foods is a serious health issue: A review. Sustainability, 14(1), 161. doi: 10.3390/su14010161.

Niu LL, Yang FX, Xu C, Yang HY, Liu WP. 2013. Status of metal accumulation in farmland soils across China: From distribution to risk assessment. Environmental Pollution, 176, 55–62. doi: 10.1016/j.envpol.2013.01.019.

Pandey B, Agrawal M, Singh S. 2014. Assessment of air pollution around coal mining area: Emphasizing on spatial distributions, seasonal variations and heavy metals, using cluster and principal component analysis. Atmospheric Pollution Research, 5(1), 79–86. doi: 10.5094/APR.2014.010.

Park HJ, Park HJ, Yang HI, Park SI, Lim SS, Kwak JH, Lee GT, Lee SM, Park M, Choi WJ. 2019. Sorption of Pb in chemical and particle-size fractions of soils with different physico-chemical properties. Journal of Soils and Sediments, 19(1), 310–321. doi: 10.1007/s11368-018-1978-3.

Peng XY, Wan F, Xie QF, Zhang X, Huang S. 2012. Numerical simulation of atmospheric migration of particles from uranium tailings impoundment. Applied Mechanics and Materials, 253–255, 1014–1018. doi: 10.4028/www.scientific.net/amm.253-255.1014.

Qiao PW, Wang S, Li JB, Zhao QY, Wei Y, Lei M, Yang J, Zhang ZG. 2023. Process, influencing factors, and simulation of the lateral transport of heavy metals in surface runoff in a mining area driven by rainfall: A review. Science of the Total Environment, 857, 159119. doi: 10.1016/j.scitotenv.2022.159119.

Rashed MN. 2010. Monitoring of contaminated toxic and heavy metals, from mine tailings through age accumulation, in soil and some wild

plants at Southeast Egypt. Journal of Hazardous Materials, 178(1-3), 739–746. doi: 10.1016/j.jhazmat.2010.01.147.

Saha A, Sen Gupta B, Patidar S, Hernández-Martínez JL, Martín-Romero F, Meza-Figueroa D, Martínez-Villegas N. 2024. A comprehensive study of source apportionment, spatial distribution, and health risks assessment of heavy metal(loid)s in the surface soils of a semi-arid mining region in Matehuala, Mexico. Environmental Research, 260, 119619. doi: 10.1016/j.envres.2024.119619.

Sawut R, Kasim N, Maihemuti B, Hu L, Abliz A, Abdujappar A, Kurban M. 2018. Pollution characteristics and health risk assessment of heavy metals in the vegetable bases of northwest China. Science of the Total Environment, 642, 864–878. doi: 10.1016/j.scitotenv.2018.06.034.

Stovern M, Rine KP, Russell MR, Félix O, King M, Eduardo Sáez A, Betterton EA. 2015. Development of a dust deposition forecasting model for mine tailings impoundments using in situ observations and particle transport simulations. Aeolian Research, 18, 155–167. doi: 10.1016/j.aeolia.2015.07.003.

Sun ZH, Xie XD, Wang P, Hu YA, Cheng HF. 2018. Heavy metal pollution caused by small-scale metal ore mining activities: A case study from a polymetallic mine in South China. Science of the Total Environment, 639, 217–227. doi: 10.1016/j.scitotenv.2018.05.176.

US EPA (United States Environmental Protection Agency). 1986. Guidelines for the health risk assessment of chemical mixtures. United States Environmental Protection Agency, Washington, DC. Fed. Reg. , 51(185), 34014–34025.

US EPA (United States Environmental Protection Agency). 1989. Risk Assessment Guidance for Superfund. Human Health Evaluation Manual (Part A). United States Environmental Protection Agency, Washington, DC. Interim Final, I, 11989.

US EPA (United States Environmental Protection Agency). 2000. Hand book for Non-Cancer Health Effects Evaluation. United States Environmental Protection Agency, Washington, DC.

US EPA (United States Environmental Protection Agency). 2004. Integrated Risk Information System (IRIS). Lead and Compounds (Inorganic) (CASRN7439-92-1).

Wang FF, Guan QY, Tian J, Lin JK, Yang YY, Yang LQ, Pan NH. 2020. Contamination characteristics, source apportionment, and health risk assessment of heavy metals in agricultural soil in the Hexi Corridor. Catena, 191, 104573. doi: 10.1016/j.catena.2020.104573.

Wang YZ, Duan XJ, Wang L. 2020. Spatial distribution and source analysis of heavy metals in soils influenced by industrial enterprise distribution: Case study in Jiangsu Province. Science of the Total Environment, 710, 134953. doi: 10.1016/j.scitotenv.2019.134953.

Wei CY, Wang C, Yang LS. 2009. Characterizing spatial distribution and sources of heavy metals in the soils from mining-smelting activities in Shuikoushan, Hunan Province, China. Journal of Environmental Sciences, 21(9), 1230–1236. doi: 10.1016/S1001-0742(08)62409-2.

Wei MC, Pan AF, Ma RY, Wang H. 2023. Distribution characteristics, source analysis and health risk assessment of heavy metals in farmland soil in Shiquan County, Shaanxi Province. Process Safety and Environmental Protection, 171, 225–237. doi: 10.1016/j.psep.2022.12.089.

Xie Q, Ren BZ, Hursthouse A, Shi XY. 2022. Effects of mining activities on the distribution, controlling factors, and sources of metals in soils from the Xikuangshan south mine, Hunan Province. Integrated Environmental Assessment and Management, 18(3), 748–756. doi: 10.1002/ieam.4514.

Yang JS, Lee JY, Baek K, Kwon TS, Choi J. 2009. Extraction behavior of As, Pb, and Zn from mine tailings with acid and base solutions. Journal of Hazardous Materials, 171(1–3), 443–451. doi: 10.1016/j.jhazmat.2009.06.021.

Yang SY, Zhou QH, Sun LJ, Qin Q, Sun YF, Wang J, Liu XM, Xue Y. 2024. Source to risk receptor transport and spatial hotspots of heavy metals pollution in peri-urban agricultural soils of the largest megacity in China. Journal of Hazardous Materials, 480, 135877. doi: 10.1016/j.jhazmat.2024.135877.

Yin ZY, Li R, Lin H, Chen YF, Wang YX, Zhao YL. 2022. Analysis of influencing factors of cementitious material properties of lead-zinc tailings based on orthogonal tests. Materials, 16(1), 361. doi: 10.3390/ma16010361.

Yu J Y, Wang JJ, Zhang W, Kattel GR, Kumar A, Yu ZG. 2024. Complexity of hydrology, sewage and industries in distribution and migration pathways of heavy metals at spatial scale of China's brown fields. Ecohydrology, 17(4), e2588. doi: 10.1002/eco.2588.

Yu JA, Chen Z, Gao WH, He S, Xiao D, Fan W, Huo MX, Nugroho WA. 2025. Global trends and prospects in research on heavy metal pollution at contaminated sites. Journal of Environmental Management, 383, 125402. doi: 10.1016/j.jenvman.2025.125402.

Yun SW, Kim DH, Kang DH, Son J, Lee SY, Lee CK, Lee SH, Ji WH, Baveye PC, Yu C. 2017. Effect of farmland type on the transport and spatial distribution of metal(loid)s in agricultural lands near an abandoned gold mine site: confirmation of previous observations. Journal of Geochemical Exploration, 181, 129–137. doi: 10.1016/j.gexplo.2017.07.004.

Zhang CQ, Liu H, Wang DH, Chen YC, Rui ZY, Lou DB, Wu Y, Jia FD, Chen ZH, Meng XY. 2015. A preliminary review on the metallogeny of Pb‐Zn deposits in China. Acta Geologica Sinica (English Edition), 89(4), 1333–1358. doi: 10.1111/1755-6724.12532.

Zhang Y, Fang Q, Lv JW, Fu YK, Zhu JH, Peng GJ, Li M, Wu XY, Wang HQ, Chen ZY. 2023. Source control on the acid mine drainage produced by the oxidation of pyrite and sulfur-containing uranium tailings based on the microbially induced carbonate precipitation technology. Journal of Cleaner Production, 428, 139444. doi: 10.1016/j.jclepro.2023.139444.

Zhang Y, Yin CB, Cao SZ, Cheng LL, Wu GS, Guo JB. 2018. Heavy metal accumulation and health risk assessment in soil-wheat system under different nitrogen levels. Science of the Total Environment, 622, 1499–1508. doi: 10.1016/j.scitotenv.2017.09.317.

Zhang YW, Liu YT, Wang ZW, Cao Y, Tu XR, Cao D, Yuan S, Cheng XM, Zhang LS. 2023. Source analysis of dissolved heavy metals in the Shaying River Basin, China. Journal of Groundwater Science and Engineering, 11(4), 408–421 doi: 10.26599/jgse.2023.9280032.

Zhang Z, Wu HF, Zhang AY, Tan MT, Yan SC, Jiang D. 2024. Transfer of heavy metals along the food chain: A review on the pest control performance of insect natural enemies under heavy metal stress. Journal of Hazardous Materials, 478, 135587. doi: 10.1016/j.jhazmat.2024.135587.

Zhao HQ, Chang RQ, Jin Q, Wu YH, Wang XF, Ma HC, Li MY, Fu HC. 2023. Spatial analysis and risk assessment of soil heavy metal pollution in the Xishimen iron mining area of Hebei Province. Rock and Mineral Analysis, 42(2), 371–382 (in Chinese). doi: 10.15898/j.cnki.11-2131/td.202203290066.

Zhou H, Yue XM, Chen Y, Liu YZ. 2024. Source-specific probabilistic contamination risk and health risk assessment of soil heavy metals in a typical ancient mining area. Science of the Total Environment, 906, 167772. doi: 10.1016/j.scitotenv.2023.167772.

Zhuang P, Yang QW, Wang HB, Shu WS. 2007. Phytoextraction of heavy metals by eight plant species in the field. Water, Air, and Soil Pollution, 184(1), 235–242. doi: 10.1007/s11270-007-9412-2.

Zhuo HM, Wang X, Liu H, Fu SZ, Song H, Ren LJ. 2020. Source analysis and risk assessment of heavy metals in development zones: A case study in Rizhao, China. Environmental Geochemistry and Health, 42(1), 135–146. doi: 10.1007/s10653-019-00313-7.